

Quantitative canvas weave analysis using 2D synchrosqueezed transforms

Haizhao Yang¹, Jianfeng Lu², William P. Brown³, Ingrid Daubechies⁴, *Fellow, IEEE*, and Lexing Ying⁵

¹Department of Mathematics, Stanford University, Stanford, CA 94305 USA

²Departments of Mathematics, Chemistry, and Physics, Duke University, Durham, NC 27708 USA

³North Carolina Museum of Art, Raleigh, NC 27607 USA

⁴Department of Mathematics, Duke University, Durham, NC 27708 USA

⁵Department of Mathematics and Institute for Computational and Mathematical Engineering, Stanford University, Stanford, CA 94305 USA

I. INTRODUCTION

QUANTITATIVE canvas weave analysis has many applications in art investigations of paintings, including dating, forensics, canvas rollmate identification [1]–[3]. Traditionally, canvas analysis is based on x-radiographs. Prior to serving as a painting canvas, a piece of fabric is coated with a priming agent; smoothing its surface makes this layer thicker between and thinner right on top of weave threads. These variations affect the x-ray absorption, making the weave pattern stand out in x-ray images of the finished painting. To characterize this pattern, it is customary to visually inspect small areas within the x-radiograph and count the number of horizontal and vertical weave threads; averages of these then estimate the overall canvas weave density. The tedium of this process typically limits its practice to just a few sample regions of the canvas. In addition, it does not capture more subtle information beyond weave density, such as thread angles or variations in the weave pattern. Application of signal processing techniques to art investigation are now increasingly used to develop computer-assisted canvas weave analysis tools.

In their pioneering work [4], Johnson *et al* developed an algorithm for canvas thread-counting based on windowed Fourier transforms (wFT); further developments in [5], [6] extract more information, such as thread angles and weave patterns. Successful applications to paintings of art historical interest include works by van Gogh [7], [8], Diego Velázquez [9], Johannes Vermeer [10], among others [11]–[15].

A more robust and automated analysis technique was later developed by Erdmann *et al* [16], based on autocorrelation and pattern recognition algorithms, requiring less human intervention (e.g., choosing proper frequency range and window size of windowed Fourier transforms). Unlike the Fourier-space based approach of [4], [16] uses only the real-space representation of the canvas. Likewise, [17] also uses real-space based features for canvas texture characterization.

We consider here a new automated analysis technique for quantitative canvas analysis, based on the 2D synchrosqueezed transforms recently developed in [18]–[20]. In this Fourier-

space based method, the nonlinear synchrosqueezing procedure is applied to a phase-space representation of the image obtained by wavepacket or curvelet transforms. Synchrosqueezing has shown to be a useful tool in independent work by some of us [18]–[22], in the general area of materials science, medical signal analysis, and seismic imaging. Using as a prior assumption that the signal of interest consists of a sparse superposition of close to but not quite periodic template functions, this mathematical tool provides sharp and robust estimates for the locally varying instantaneous frequencies of the signal components, by exploiting the phase information of wFT (*i.e.*, not only the absolute value as in previous methods). This seemed to make it a natural candidate for canvas analysis; as illustrated by the results we obtained, reported here, this intuition proved to be correct. The method, as shown below, is very robust and offers fine scale weave density and thread angle information for the canvas. We compare our results with those in [4]–[6], [16].

We explain our model for x-radiography images for canvas analysis in Section II; the use and limitations of windowed Fourier transforms are discussed in Section III-A. Section III-B introduces the synchrosqueezed transform, with applications to quantitative canvas analysis; section IV presents various examples, applying our technique in art investigation.

II. MODEL OF THE CANVAS WEAVE PATTERN IN X-RADIOGRAPHY

We denote by f the intensity of an x-radiograph of a painting; see Figure 1a for a (zoomed-in) example. Because x-rays penetrate deeply, the image consists of several components: the paint layer itself, primer, canvas (if the painting is on canvas or on wood panel overlaid with canvas), possibly a wood panel (if the painting is on wood), and sometimes extra slats (stretchers for a painting on canvas, or a cradle for a painting on wood, thinned and cradled according to earlier conservation practice.) This x-ray image may be affected by noise or artifacts of the acquisition process. We model the intensity function f as an additive superposition of the canvas contribution, denoted by $c(x)$, and a remainder, denoted by $p(x)$, that incorporates all the other components. Our approach to quantitative canvas

analysis relies on a simple model for the x-ray image of the weave pattern in the “ideal” situation. Since it is produced by the interleaving of horizontal and vertical threads in a periodic fashion, a natural general model is

$$f(x) = c(x) + p(x) := a(x)S(2\pi N\phi(x)) + p(x). \quad (1)$$

In this expression, S is a periodic function on the square $[0, 2\pi)^2$, the details of which reflect the basic weave pattern of the canvas, e.g., whether it is a plain weave or perhaps a twill weave. This is a generalization of more specific assumptions used in the literature – for instance, in [4] plain weave canvas is modeled by taking for S a sum of sinusoidal functions in the x and y directions; in [6], more general weave patterns (in particular twill) are considered. The parameter N in (1) gives the averaged overall weave density of the canvas (in both directions). The function ϕ , which maps the image domain to \mathbb{R}^2 , is a smooth deformation representing the local warping of the canvas; it contains information on local thread density, local thread angles, etc. The slowly varying function $a(x)$ accounts for variations of the amplitude of the x-ray image of the canvas, e.g., due to variation in illumination conditions.

In some cases, the x-ray image fails to show canvas information in portions of the painting (e.g. when the paint layer dominates); the model (1) is then not uniformly valid. Because our analysis uses spatially localized information (analyzing the image patch by patch), this affects our results only locally: in those (small) portions of the image we have no good estimates for the canvas parameters. For simplicity, this exposition assumes that (1) is valid for the whole image.

We rewrite c by representing the weave pattern function S , periodic on $[0, 2\pi)^2$, in terms of its Fourier series,

$$c(x) = \sum_{n \in \mathbb{Z}^2} a(x)\widehat{S}(n)e^{2\pi i N n \cdot \phi(x)}. \quad (2)$$

This is a superposition of smoothly warped plane-waves with local wave vectors $N\nabla(n \cdot \phi(x))$. The idea of our analysis is to extract the function ϕ by exploiting that the Fourier coefficients $\{\widehat{S}(n)\}$ are dominated by a few leading terms.

III. FOURIER-SPACE BASED CANVAS ANALYSIS

A. Windowed Fourier transform

Because a and ϕ vary slowly with x , we can use Taylor expansions to approximate the function for x near x_0 as

$$c(x) \approx \sum_{n \in \mathbb{Z}^2} a(x_0)\widehat{S}(n)e^{2\pi i N n \cdot \phi(x_0)} e^{2\pi i N(x-x_0) \cdot \nabla_x(n \cdot \phi)(x_0)}. \quad (3)$$

The right hand side of (3) is a superposition of complex exponentials with frequencies $w = (w_1, w_2)$, with

$$w_l = \sum_{\nu=1}^2 n_\nu (\partial_\nu \phi_\nu)(x_0);$$

these would stand out in a Fourier transform as peaks in the 2-dim Fourier spectrum. Since the approximation is accurate only near x_0 , we also use a windowed Fourier transform with

envelope given by, e.g., a Gaussian centered at x_0 with width σ . We have then

$$\begin{aligned} W(x_0, k) &:= \frac{1}{2\pi\sigma^2} \iint e^{-2\pi i k(x-x_0)} e^{-(x-x_0)^2/2\sigma^2} c(x) d^2x \\ &\approx \sum_{n \in \mathbb{Z}^2} a(x_0)\widehat{S}(n)e^{2\pi i N n \cdot \phi(x_0)} e^{-2\pi^2 \sigma^2 [k - N\nabla_x(n \cdot \phi)(x_0)]^2}. \end{aligned} \quad (4)$$

Instead of being sharply peaked, the spectrum of the windowed Fourier transform is thus “spread out” around the $N\nabla_x(n \cdot \phi)(x_0)$ – a manifestation of the well-known uncertainty principle in signal processing, with a trade-off w.r.t. the parameter σ : a larger σ reduces the “spreading” at the price of a larger error in the approximation (3), since the Gaussian is then correspondingly wider in the real space.

The method of [4], [6] uses the local maxima of the amplitude of the windowed Fourier transform to estimate the location of $\{N\nabla(n \cdot \phi(x_0))\}$ for a selection of positions x_0 of the x-ray image (local swatches are used instead of the Gaussian envelope, but the spirit is the same). For ideal signals, (4) shows that the maxima of the amplitude $|W(x_0, \cdot)|$ identify the dominating wave vectors in Fourier-space, which are then used to extract information, including weave density and thread angles. Thread density is estimated by the length of the wave vectors; the weave orientation is determined by the angles. This back-of-the-envelope calculation is fairly precise when N is much larger than 1, resulting in a small $\mathcal{O}(N^{-1})$ error in the Taylor expansions and stationary phase approximations. In terms of the canvas, $N \gg 1$ means that the inverse of the average thread density must be much smaller than the length scale of the variation of the canvas texture, which is typically on the scale of the size of the painting. This is essentially a high-frequency assumption, ensuring that stationary phase approximations can be applied in the time-frequency analysis. Details can be found in standard references of time-frequency analysis, e.g., the book [23].

In more complicated scenarios, in particular, when the x-ray signal corresponding to the canvas is heavily “contaminated” by the other parts of the painting, it is desirable to have more robust and refined analysis tools at hand than locating local maxima of the Fourier spectrum. The synchrosqueezed transforms are nonlinear time-frequency analysis tools developed for this purpose, in different (1D and 2D) applications which suggests they could be suitable for canvas analysis in challenging situations. A comparison of the two methods is shown in Figure 1 and will be explained below. For the sake of completeness, we note that in our implementation, we use curvelets (more or less corresponding to a non-isotropic Gaussian window, with axes-lengths adapted to the frequencies of the oscillating component) rather than windowed Fourier transforms with isotropic Gaussian windows, to which we have restricted ourselves in this exposition. The synchrosqueezing operation has similar effects in both cases; the curvelet implementation, while more complicated to explain in a nutshell, has the advantage of being governed by only two parameters, which set the spatial redundancy and the angular resolution. Setting these is well understood (see [24]); in addition the result is stable under small perturbations in these parameters.

B. Synchrosqueezed transforms

The synchrosqueezed transforms, or more generally time-frequency reassignment techniques (see e.g., the recent review [25]), were introduced to deal with the “loss of resolution” due to the uncertainty principle. Originally introduced in [26] for auditory signals, using a nonlinear squeezing of the time-frequency representation to gain sharpness of the time-frequency representation, the 1D synchrosqueezed wavelet transform was revisited and analyzed in [27]. For the application to canvas analysis, we rely on 2D extensions of the synchrosqueezing transforms based on wavepacket and curvelet transforms [18], [19]. This 2D synchrosqueezing transform (2DST) has been applied to atomic-resolution crystal image analysis in [20]; the present algorithm for canvas analysis is adapted from [20], where the 2DST proved to be an excellent tool to capture and quantify deviations from a perfect lattice structure, very similar to the aims of canvas analysis. Rigorous robustness analysis of the synchrosqueezed transforms in [24] supports their application to canvas analysis where data is usually noisy and contains contaminants.

The crucial observation is that the phase of the complex function $W(x, k)$, obtained from the windowed Fourier transform (4) contains information on the local frequency (i.e., the instantaneous frequency) of the signal. Indeed, for (x, k) such that k is close to $N\nabla_x(n \cdot \phi)$, we have

$$w_f(x, k) := \frac{1}{2\pi} \Im (\nabla_x \ln W(x, k)) = N\nabla_x(n \cdot \phi)(x) + o(N), \quad (5)$$

where $\Im(z)$ stands for the imaginary part of the complex number z . Motivated by this heuristic, the synchrosqueezed windowed Fourier transform “squeezes” the time-frequency spectrum by reassigning the amplitude at (x, k) to $(x, w_f(x, k))$ as

$$T(x, \xi) := \iint |W(x, k)|^2 \delta(\xi - w_f(x, k)) d^2k. \quad (6)$$

This significantly enhances the sharpness of the time-frequency representation, leading to an estimate of the local frequency of the signal, that is more accurate as well as more robust, as we illustrate below. This gives a sharpened energy distribution on phase space:

$$T(x, \xi) \approx \sum_{n \in \mathbb{Z}^2} |a(x)|^2 |\widehat{S}(n)|^2 \delta(\xi - N\nabla(n \cdot \phi(x))), \quad (7)$$

in the sense of distributions. See [18]–[20] for more details, as well as an analysis of the method. The peaks of the synchrosqueezed spectrum T then provide estimates of the $N\nabla(n \cdot \phi(x))$, determining local measurement of both the thread count and the angle. Figure 1 illustrates the resulting spectrum of the 2DST, compared with the wFT for a sample x-ray image from a canvas. The reassignment carried out in (6), taking into account the local oscillation of the phase of a highly redundant wFT rather than the maximum energy of the wFT to reduce the influence of noise, results in a much more concentrated spatial frequency portrait. As illustrated by the behavior of the estimates when extra noise is added, this leads to increased robustness for the estimates of the dominating wave vectors, which determine the thread count and angle. The

performance and the robustness of the 2DST are supported by rigorous mathematical analysis in [24].

IV. APPLICATIONS TO ART INVESTIGATIONS

Let us now present some results of quantitative canvas analysis using 2DST. The algorithm is implemented in `Matlab`. The codes are open source and available as `SynLab` at <https://github.com/HaizhaoYang/SynLab>.

The first example (Fig. 2a) is the painting F205 by van Gogh, the x-ray image of which is publicly available as part of the RKD dataset [28] provided by the Netherlands Institute for Art History; this was one of the first examples analyzed using the method based on the windowed Fourier transform; see [4, Figure 4] and also [6, Figure 6]. In Figure 3, the thread count and thread angle estimates are shown for horizontal and vertical threads. Comparing with the previous results in [4], [6], we observe that the general characteristics of the canvas agree quite well. For example, [6] reports average thread counts of 13.3 threads/cm (horizontal) and 16.0 threads/cm (vertical), while our method obtains 13.24 threads/cm (horizontal) and 15.92 threads/cm (vertical). Compared to the earlier results, the current analysis gives a more detailed spatial variation of the thread counts. In particular, it captures the oscillation of the thread count on a much finer scale. We don’t know whether such fine details will have applications beyond the canvas characterization already achieved by less detailed methods, but it is interesting that they can be captured by an automatic method. Note that visual inspection confirms the presence of these fine details.

We next consider a painting of Vermeer, *Woman in Blue Reading a Letter* (L17), the x-ray image of which is also available as part of the RKD dataset [28]. The canvas analysis for Vermeer’s paintings is considerably more challenging than that of van Gogh’s [10]. This can be understood by direct comparison of the x-ray images in Figures 2b and 2a. The stretchers and nails significantly perturb the x-ray image for the Vermeer. The results are shown in Figures 4 and 5. Although the thread count and angle estimate are affected by artifacts in the x-ray image, they still provide a detailed characterization of the canvas weave. This is justified by the result in Figure 5, which shows a zoom-in for the x-ray image and the vertical thread angle map. It is observed that the algorithm captures (and quantifies) detailed deviations in the vertical thread angle recognizable by visual inspection. Despite the challenges, the 2DST-based canvas analysis performs quite well on the Vermeer example.

To test the algorithm on a different type of canvas weave, we applied it to the x-ray image of Albert P. Ryder’s *The Pasture*, a painting on twill canvas. Figure 6 shows the result for a portion of the canvas. The twill canvas pattern is clear on the zoomed-in x-ray image. The method is still able to capture fine scale features of the canvas; the admittedly higher number of artifacts is due to the increased difficulty to “read” a twill vs. a standard weave pattern, as well as a weaker canvas signal on the x-ray.

For our final example, we apply the 2DST-based canvas analysis to *The Peruzzi Altarpiece* by Giotto di Bondone and

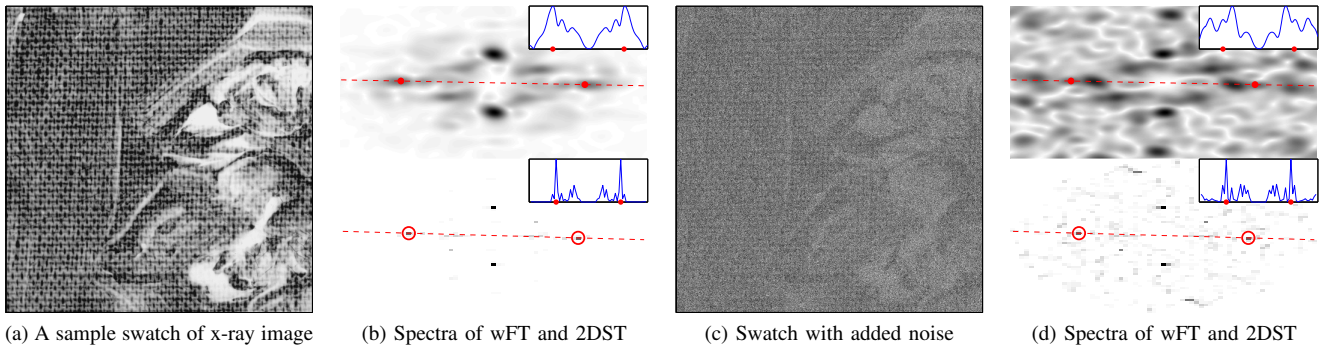


Fig. 1. (a) A sample swatch of an x-ray image, in which canvas is clearly visible (in most places) despite the paint layers on top of the canvas; (b) The spectrum of the windowed Fourier transform (wFT) (top) and 2DST (bottom) at one location. Local maxima (circled in red) indicate the wave vector estimates; the insets show the intensity profile on a cross section (dashed line) through two maxima; (c) The same swatch as in (a) with noise added (such that the noise level is visually comparable to the real data example in Figure 8) to test for robustness; (d) The wFT and 2DST spectra again at the same location, illustrating the more robust nature of the 2DST estimate (due to its taking into account phase information of the wFT in a neighborhood of the peaks of the absolute value of the wFT as well as the peak values). For comparison, the positions of the red circles are the same as in (b). The peaks are displaced in wFT due to noise, while the result of 2DST is not affected.

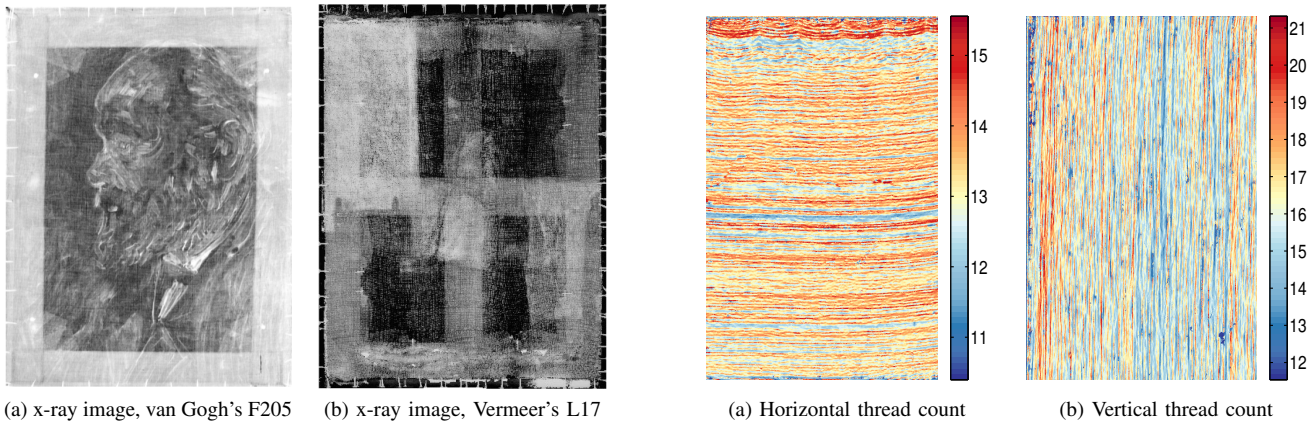


Fig. 2. (a) X-ray image of van Gogh’s painting *Portrait of an Old Man with Beard*, 1885, Van Gogh Museum, Amsterdam (F205); (b) X-ray image of Vermeer’s painting *Woman in Blue Reading a Letter*, 1663-64, Rijksmuseum Amsterdam, Amsterdam (L17). X-ray images provided by Professor C. Richard Johnson through the RKD dataset [28].

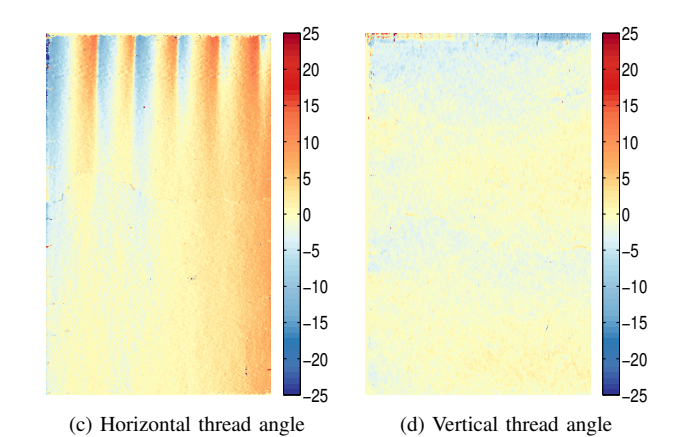


Fig. 3. The canvas analysis results of van Gogh’s F205 using the synchrosqueezed transform: (a) and (b): thread count map of the horizontal and vertical threads; (c) and (d): the estimated thread angle. Compare with [6, Figure 6].

his assistants. The altarpiece is in the collection of the North Carolina Museum of Art; see Figure 7 for the altarpiece as well as the x-ray images used in the analysis. This is a painting on wood panel, but the ground of traditional white gesso was applied over a coarsely woven fabric interlayer glued to a poplar panel. We carried out a canvas analysis on the fabric interlayer, likely a hand woven linen cloth. The results of a canvas analysis based on the synchrosqueezed transform are shown in Figure 9. This example is much more challenging than the previous ones, since the x-ray intensity contributed by the canvas is much weaker because the ground does not contain lead; see e.g., Figure 8, a detail of the x-ray image of the Christ panel. The canvas is barely visible, in sharp contrast to the x-ray images in, e.g., Figures 1a or 5. All panels except the central Christ panel are cradled; the wood texture of these cradles interferes with the canvas pattern on the x-ray image, introducing an additional difficulty. This difficulty is reflected in our results: e.g., the vertical thread count for the central panel has much fewer artifacts than those of the other panels (see Figure 9). [In future work, we will explore carrying out a canvas analysis after signal-processing-based virtual cradle removal – see [29].]

One interesting ongoing art investigation debate concerning this altarpiece is the relative position of the panels of John the Baptist and Francis of Assisi. While the order shown in Figure 7, with Francis in the right-most position, and the Baptist second from right, is the most commonly accepted [30], there have been alternative arguments that the Francis panel should be instead placed next to the central panel. Typically the grain of the wood as seen in x-rays can be used to set the relative position of panels in an altarpiece painted on

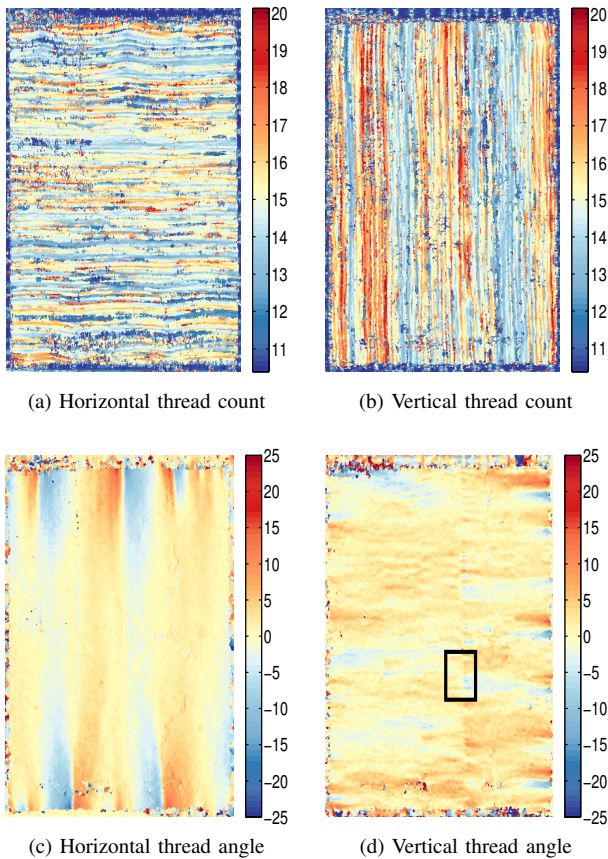


Fig. 4. Canvas analysis results of Vermeer’s L17 using the synchrosqueezed transform: (a) and (b) are thread count map of the horizontal and vertical threads; (c) and (d) show the estimated thread angle. Average thread density is 14.407 threads/cm (horizontal) and 14.817 threads/cm (vertical). The boxed region of the vertical thread angle map (panel (d)) is shown, enlarged, in Figure 5; it is part of a striking anomaly in the vertical angle pattern in this canvas, lining up along one vertical traversing the whole canvas.

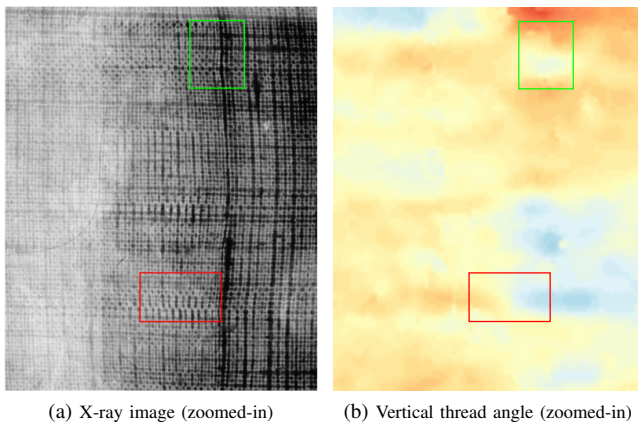


Fig. 5. Details of the x-ray image and the corresponding vertical thread angle map for Vermeer’s L17, highlighting two examples (boxed regions) of noticeable fine scale variation of the vertical thread angle, readily recognizable also by visual inspection of the corresponding zones in the x-ray image.

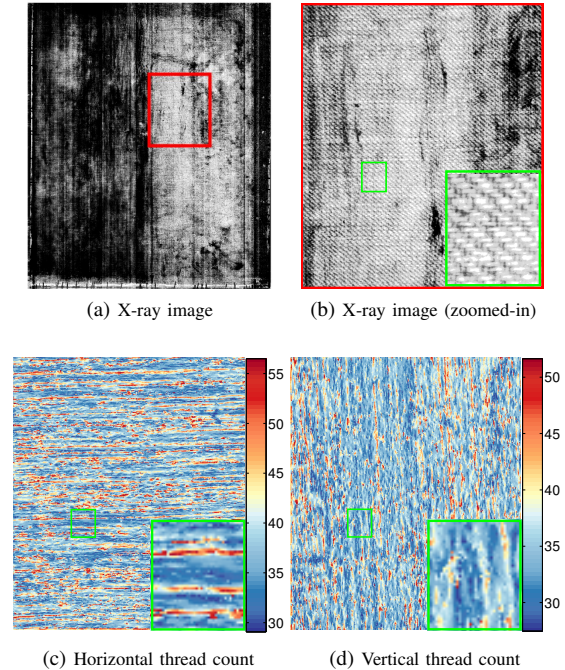


Fig. 6. (a) X-ray image of Albert P. Ryder’s *The Pasture*, 1880-85, North Carolina Museum of Art, Raleigh. (b) is an enlargement of the red-boxed region, with clearly recognizable twill canvas weave. (c) and (d) show the thread count maps corresponding to the zoomed-in region shown in (b). Note the much higher thread counts than for plain weave canvas, typical for the finer threads used in twill weave. The bottom-right insets of (b), (c) and (d) show the further zoom-in of the green-boxed region for visual inspection. The horizontal thread count matches the changes observed in the x-ray image quite well.

a single plank of wood, but because the cradle pattern obscures an accurate reading of the x-rays of the Baptist and Francis this proposed alternative orientation can not be discounted. We wondered what ordering (if any) would be suggested by the canvas analysis. Under the assumption that the pieces of canvas are cut off consecutively from one larger piece of cloth, we investigated which arrangement provides the best matching. One plausible arrangement of the canvas is shown in Figure 10. Our analysis suggests that the canvas of the central panel should be rotated for 90 degrees clockwise to match with the other panels. (The larger height of the central panel, possibly exceeding the width of the cloth roll, may have necessitated this.) Moreover, a better matching is achieved if the canvas of the panel of the Baptist is flipped horizontally (in other words, flipped front to back). Given our results, it seems unlikely that the Francis-panel canvas would fit best to the left of the Baptist-panel canvas. A better, more precise result will be possible after virtual cradle removal. Of course, even a more thorough canvas roll arrangement would not be conclusive evidence for the relative position of the panels themselves; but combined with other elements in a more exhaustive study, it can play a significant role.

V. CONCLUSION

We apply 2D synchrosqueezed transforms to quantitative canvas weave analysis for art investigations. The synchrosqueezed transforms offer a sharpened phase-space representation of the x-ray image of the paintings, which yields

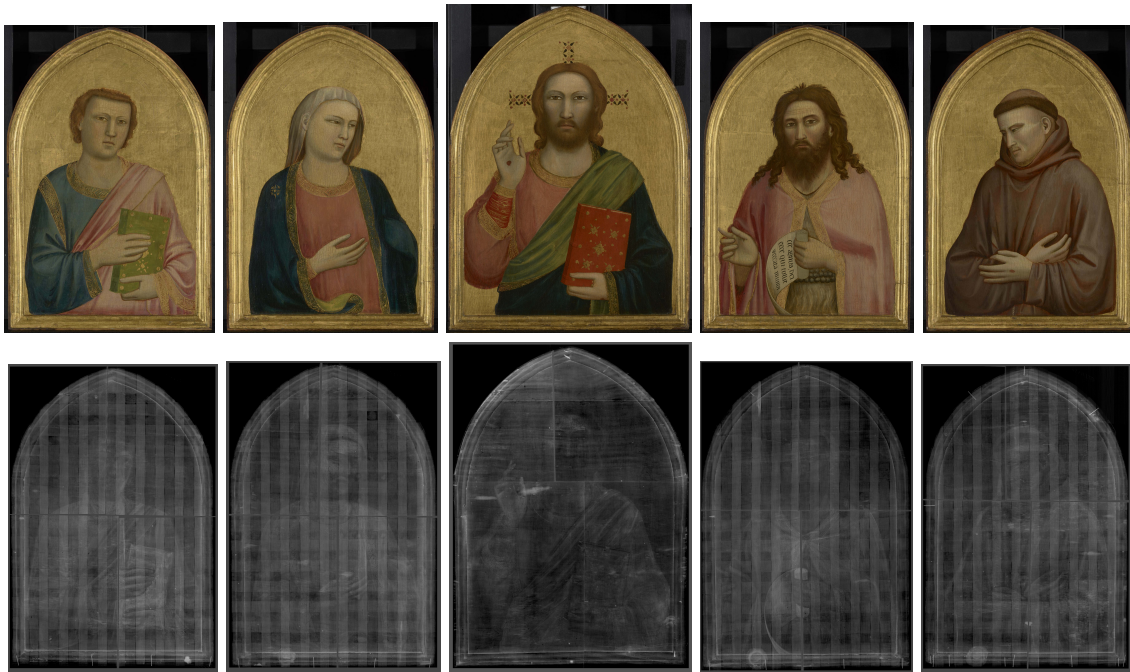


Fig. 7. Giotto di Bondone and assistants, *The Peruzzi Altarpiece*, ca. 1310-15, North Carolina Museum of Art, Raleigh. The panels from left to right are John the Evangelist, the Virgin Mary, Christ in Majesty, John the Baptist, and Francis of Assisi. The resolution of the x-ray image used in the analysis is 300 DPI. The vertical and (less obvious) horizontal stripes on the x-ray images in all panels except the central panel of Christ are caused by cradling. Each x-ray image is a mosaic of 4 x-ray films, leading to visible boundaries of the different pieces (thin horizontal and vertical lines) on the x-ray image.

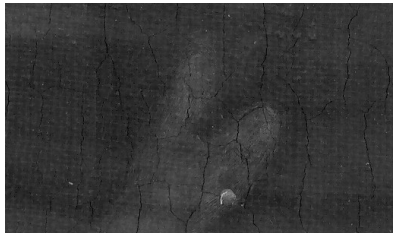


Fig. 8. A zoomed-in x-ray image of the central panel in *The Peruzzi Altarpiece*. The canvas texture is barely visible, even though the image is scaled such that the thread density is comparable with that of the zoomed-in x-ray in Figure 5.

fine scale characterization of thread count and thread angle of the canvas. We demonstrated the effectiveness of the method on art works by van Gogh, Vermeer, and Ryder. The tool is applied to *The Peruzzi Altarpiece* by Giotto and his assistants, to provide insight into the issue of panel arrangement.

ACKNOWLEDGMENT

We are grateful to C. Richard Johnson, Jr. for providing x-ray images in the RKD dataset and for his help and encouragement throughout this project. We would like to thank Bruno Cornelis and Rachel Yin for helpful discussions. We thank Noelle Ocon, Conservator of Paintings at North Carolina Museum of Art, for mozaicing Giotto x-rays and also John Taormina, Director of Visual Media Center at Duke University, for assistance in scanning the x-ray film of *The Pasture* by Albert P. Ryder. The work of I.D. was partly supported by a grant from AFOSR and by NSF award DMS-1320655. The work of J.L. was supported in part by the Alfred P. Sloan Foundation and the National Science Foundation under award DMS-1312659. The work of H.Y. and L.Y. was partially supported by the National Science Foundation under award

DMS-1328230 and the U.S. Department of Energy Advanced Scientific Computing Research program under award DE-FC02-13ER26134/DE-SC0009409.

REFERENCES

- [1] K. Lister, C. Peres, and I. Fiedler, "Appendix: tracing an interaction: supporting evidence, experimental grounds," in *Van Gogh and Gauguin: The Studio of the South*, D. Druick and P. Zegers, Eds. Thames & Hudson, 2001, pp. 354–369.
- [2] E. van de Wetering, *Rembrandt: The Painter at Work*. Amsterdam: Amsterdam University Press, 1997.
- [3] A. Kirsh and R. Levenson, *Seeing through Paintings: Physical Examination in Art Historical Studies*. Yale University Press, 2000.
- [4] D. Johnson, C. R. Johnson Jr., A. Klein, W. Sethares, H. Lee, and E. Hendriks, "A thread counting algorithm for art forensics," in *Digital Signal Processing Workshop and 5th IEEE Signal Processing Education Workshop, 2009. DSP/SPE 2009. IEEE 13th*, Jan 2009, pp. 679–684.
- [5] D. H. Johnson, R. G. Erdmann, and C. R. Johnson Jr., "Whole-painting canvas analysis using high- and low-level features," in *Proc. 36th Int. Conf. on Acoustics, Speech and Signal Processing*, 2011, pp. 969–972.
- [6] D. H. Johnson, C. R. Johnson Jr., and R. G. Erdmann, "Weave analysis of paintings on canvas from radiographs," *Signal Process.*, vol. 93, pp. 527–540, 2013.
- [7] E. Hendriks, L. Jansen, J. Salvant, E. Ravaud, M. Eveno, M. Menu, I. Fielder, M. Geldof, L. Megens, M. van Bommel, C. R. Johnson Jr., and D. H. Johnson, "A comparative study of Vincent van Gogh's Bedroom Series," in *Studying Old Master Paintings: Technology and Practice - The National Gallery Technical Bulletin 30th Anniversary Conference Postprints*, M. Spring, Ed. Archetype Publications, 2011, pp. 237–243.
- [8] L. van Tilborgh, T. Meedendorp, E. Hendriks, D. H. Johnson, C. R. Johnson Jr., and R. G. Erdmann, "Weave matching and dating of van Gogh's paintings: An interdisciplinary approach," *The Burlington Magazine*, vol. CLIV, pp. 112–122, 2012.
- [9] P. P. D'Ors, C. R. Johnson Jr., and D. H. Johnson, "Velazquez in Fraga: a new hypothesis about the portraits of El Primo and Philip IV," *The Burlington Magazine*, vol. CLIV, pp. 620–625, 2012.
- [10] W. Liedtke, C. R. Johnson Jr., and D. H. Johnson, "Canvas matches in Vermeer: A case study in the computer analysis of fabric supports," *Metropolitan Museum Journal*, vol. 47, pp. 99–106, 2012.
- [11] D. H. Johnson, E. Hendriks, and C. R. Johnson Jr., "Interpreting canvas weave matches," *Art Matters*, vol. 5, pp. 53–61, 2013.

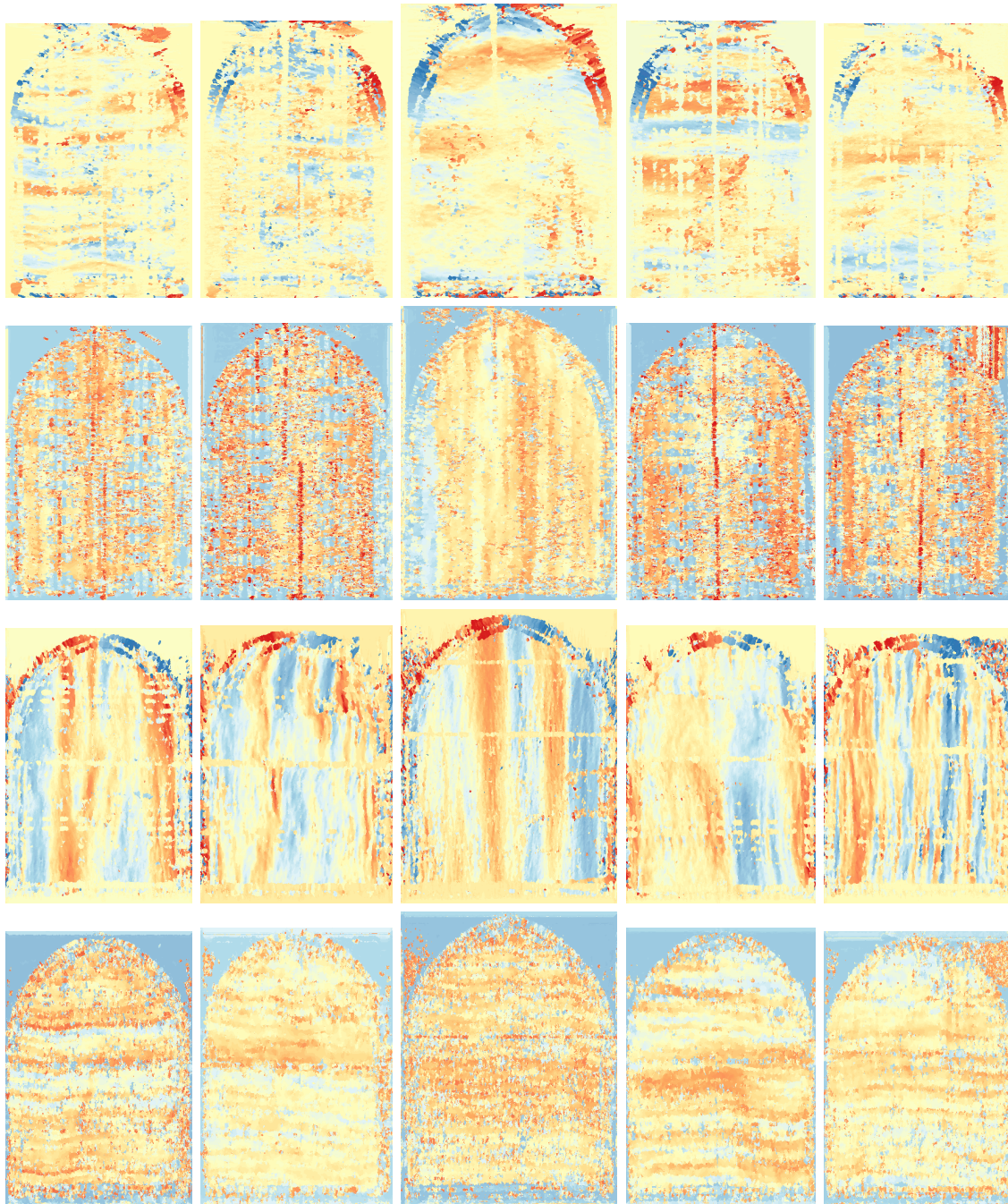


Fig. 9. Canvas analysis result of the Giotto altarpiece. First row: deviation of vertical thread angle; second row: deviation of vertical thread count; third row: deviation of horizontal thread angle; fourth row: deviation of horizontal thread count. The panels are in the same order as in Figure 7.

- [12] C. R. Johnson Jr., D. H. Johnson, I. Verslype, R. Lugtigheid, and R. G. Erdmann, "Detecting weft snakes," *Art Matters*, vol. 5, pp. 48–52, 2013.
- [13] C. R. Johnson Jr., E. Hendriks, P. Noble, and M. Franken, "Advances in computer-assisted canvas examination: Thread counting algorithms," in *37th Annual Meeting of American Institute for Conservation of Historic and Artistic Works*, Los Angeles, CA, May 2009.
- [14] D. H. Johnson, E. Hendriks, M. Geldof, and C. R. Johnson Jr., "Do weave matches imply canvas roll matches?" in *38th Annual Meeting of American Institute for Conservation of Historic and Artistic Works*, Milwaukee, WI, May 2010.
- [15] C. R. Johnson Jr., D. H. Johnson, N. Hamashima, H. S. Yang, and E. Hendriks, "On the utility of spectral-maximum-based automated thread counting from X-rays of paintings on canvas," *Studies in Conservation*, vol. 56, pp. 104–114, 2011.
- [16] R. Erdmann, C. R. Johnson Jr., M. Schafer, and J. Twilley, "Reuniting Poussin's Bacchanals painted for Cardinal Richelieu through quantitative canvas weave analysis," in *41st Annual Meeting of American Institute for Conservation of Historic and Artistic Works*, Indianapolis, IN, May 2013.
- [17] B. Cornelis, A. Doods, A. Munteanu, J. Cornelis, and P. Schelkens, "Experimental study of canvas characterization for paintings," *Proc. SPIE*, vol. 7531, p. 753103, 2010.
- [18] H. Yang and L. Ying, "Synchrosqueezed wave packet transform for 2D mode decomposition," *SIAM J. Imaging Sci.*, vol. 6, pp. 1979–2009, 2013.
- [19] —, "Synchrosqueezed curvelet transform for two-dimensional mode decomposition," *SIAM J. Math. Anal.*, vol. 46, no. 3, pp. 2052–2083, 2014.
- [20] H. Yang, J. Lu, and L. Ying, "Crystal image analysis using 2d synchrosqueezing transforms," 2014, preprint. [Online]. Available: <http://arxiv.org/abs/1402.1262>
- [21] H.-T. Wu, S.-S. Hseu, M.-Y. Bien, Y. R. Kou, and I. Daubechies, "Eval-

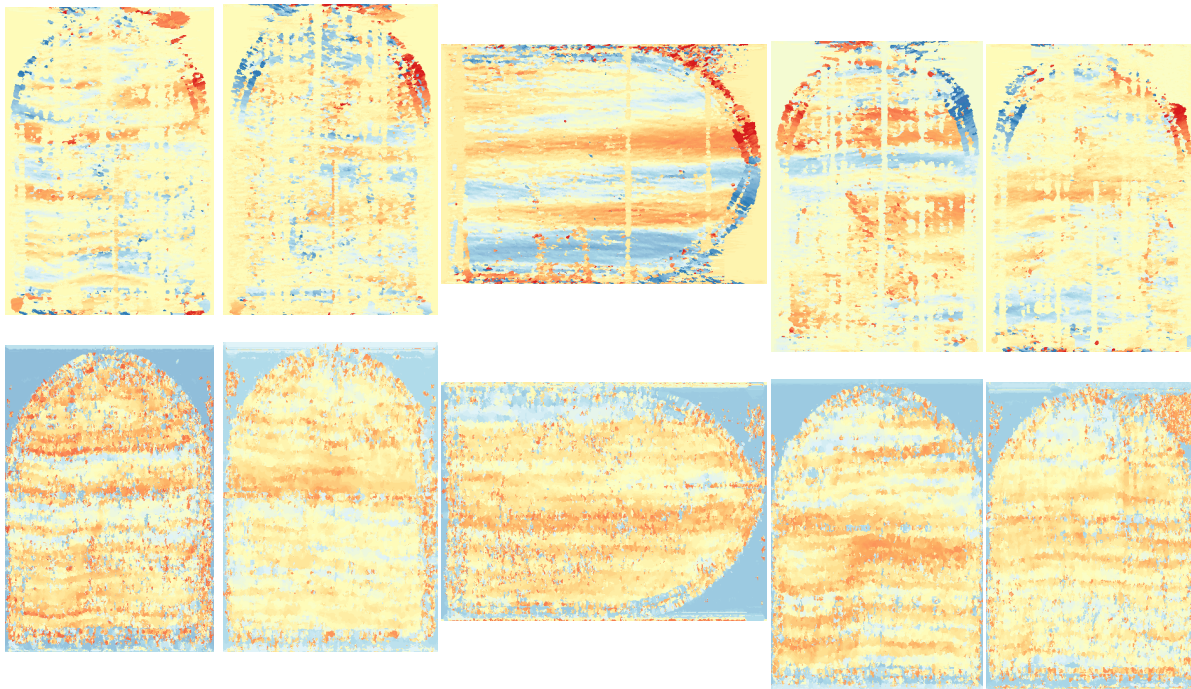


Fig. 10. A candidate canvas matching and arrangement for *The Peruzzi Altarpiece* by Giotto and his assistants. Top row: deviation of weft thread angle. Bottom row, deviation of warp thread count. (The weft thread count and warp thread angle are not shown as they are less helpful in inferring a possible arrangement.) The canvas pieces from left to right correspond to the panels for John the Evangelist, the Virgin Mary, Christ in Majesty, John the Baptist, and Francis of Assisi (in that order). The canvas of the central panel is rotated clockwise by 90 degrees, and that of the Baptist is flipped horizontally.

uating the physiological dynamics via synchrosqueezing: Prediction of the ventilator weaning,” *IEEE Trans. Biomed. Eng.*, vol. 61, no. 3, pp. 736–744, 2014.

- [22] Y.-T. Lin, H.-T. Wu, J. Tsao, H.-W. Yien, and S.-S. Hseu, “Time-varying spectral analysis revealing differential effects of sevoflurane anesthesia: nonrhythmic to rhythmic ratio,” *Acta. Anaesthesiol. Scand.*, vol. 58, no. 2, pp. 157–167, 2014.
- [23] P. Flandrin, *Time-Frequency / Time-Scale Analysis*. London: Academic Press, 1998.
- [24] H. Yang and L. Ying, “Robustness analysis of synchrosqueezed transforms,” 2014, preprint. [Online]. Available: <http://arxiv.org/abs/1410.5939>
- [25] F. Auger, P. Flandrin, Y.-T. Lin, S. McLaughlin, S. Meignen, T. Oberlin, and H.-T. Wu, “Time-frequency reassignment and synchrosqueezing: An overview,” *IEEE Signal Process. Mag.*, vol. 30, pp. 32–41, 2013.
- [26] I. Daubechies and S. Maes, “A nonlinear squeezing of the continuous wavelet transform based on auditory nerve models,” in *Wavelets in Medicine and Biology*, A. Aldroubi and M. Unser, Eds. CRC Press, 1996, pp. 527–546.
- [27] I. Daubechies, J. Lu, and H.-T. Wu, “Synchrosqueezed wavelet transforms: an empirical mode decomposition-like tool,” *Appl. Comp. Harmonic Anal.*, vol. 30, pp. 243–261, 2011.
- [28] RKD (Netherlands Institute for Art History), “Image sharing.” [Online]. Available: <http://english.rkd.nl/Services/image-sharing>
- [29] R. Yin, D. Dunson, B. Cornelis, W. Brown, N. Ocon, and I. Daubechies, “Digital cradle removal in x-ray images of art paintings,” in *IEEE International Conference on Image Processing*, Paris, Oct 2014.
- [30] D. Steel, “Catalogue entry: I. Giotto and his workshop, ‘Christ Blessing with Saint John the Evangelist, the Virgin Mary, Saint John the Baptist, and Saint Francis (Peruzzi Altarpiece),’” in *Florence at the Dawn of the Renaissance, Painting and Illumination: 1300-1350*, C. Sciacca, Ed. The J. Paul Getty Museum, 2012, pp. 24–28.

Haizhao Yang (haizhao@math.stanford.edu) is currently a Ph.D. student in the Mathematics Department at Stanford University. Before studying at Stanford University, he received the B.S. degree from Shanghai Jiao Tong University in 2010 and the M.S. degree from the University of Texas at Austin in 2012 both in mathematics.

Jianfeng Lu (jianfeng@math.duke.edu) is an Assistant Professor of Mathematics, Chemistry, and Physics at Duke University. He received the B.S. degree in mathematics from Peking University in 2005 and the Ph.D. degree in applied mathematics from Princeton University in 2009. Before joining Duke University in 2012, he was a Courant Instructor at New York University.

William P. Brown (william.p.brown@ncdcr.gov) is currently Chief Conservator of the Art Conservation Center of the North Carolina Museum of Art where he is responsible for the long-term preservation of the collection. Two years ago he established the Art+Science Initiative with Duke University to better understanding the application and degradation of artist materials. He received his M.A. and Certificate of Advanced Studies in Conservation from State University College at Buffalo, NY in 1989. Before studying at Buffalo, he received his B.A. degree from the University of Virginia in 1978.

Ingrid Daubechies (ingrid@math.duke.edu) is a James B. Duke Professor of Mathematics at Duke University. She received her B.S. and Ph.D. degrees in Physics for the Vrije Universiteit Brussel (Belgium), where she also started her research career. In the USA, she has previously been at AT&T Bell Labs (1987-94), at Rutgers University (1991-93) and at Princeton (1994-2010). She is a Fellow of the IEEE. She received the Benjamin Franklin Medal for Electrical Engineering and the James Kilby Medal of the IEEE Signal Processing Society, both in 2011.

Lexing Ying (lexing@stanford.edu) is a Professor of Mathematics at Stanford University. He received the B.S. degree from Shanghai Jiao Tong University in 1998 and the Ph.D. degree from New York University in 2004. He was a postdoctoral scholar in California Institute of Technology from 2004 to 2006. Before joining Stanford University in Dec 2012, he was a faculty member at Department of Mathematics at the The University of Texas at Austin between 2006 and 2012.